SIAM J. NUMER. ANAL.
Vol. 42, No. 1, pp. 409–433


# PERFECTLY MATCHED LAYERS FOR THE CONVECTED HELMHOLTZ EQUATION*

E. BÉCACHE†, A.-S. BONNET-BEN DHIA‡, AND G. LEGENDRE§

**Abstract.** In this paper, we propose and analyze perfectly matched absorbing layers for a problem of time-harmonic acoustic waves propagating in a duct in the presence of a uniform flow. The absorbing layers are designed for the pressure field, satisfying the convected scalar Helmholtz equation. A difficulty, compared to the Helmholtz equation, comes from the presence of so-called inverse upstream modes which become unstable, instead of evanescent, with the classical Bérenger's perfectly matched layers (PMLs). We investigate here a PML model, recently introduced for time-dependent problems, which makes all outgoing waves evanescent. We then analyze the error due to the truncation of the domain and prove that the convergence is exponential with respect to the size of the layers for both the classical and the new PML models. Numerical validations are finally presented.

**Key words.** acoustic waves, convected Helmholtz equation, duct modes, absorbing layers, perfectly matched layer, instabilities

**AMS subject classifications.** 35J05, 65N12, 76Q05

**DOI.** 10.1137/S0036142903420984

## 1. Introduction.

Perfectly matched layers (PMLs) were introduced by Bérenger [3] in order to design efficient numerical absorbing boundary conditions (more precisely, absorbing layers) for the computation of time-dependent solutions of Maxwell's equations in unbounded domains. They have since been used for numerous applications, mostly in the time domain [4, 28, 5, 23] but also for time-harmonic wave-like equations [27, 15].

In particular, PMLs have been used for the solution in the time domain of the linearized Euler equations [19, 13, 16, 26], which model acoustic propagation in the presence of a flow. In this case, it has been observed that PMLs can lead to instabilities, due to the presence of waves whose phase and group velocities have opposite signs [26] (see [2] for a general analysis of this phenomenon). Some techniques have been developed to overcome this difficulty, making the layers stable but, unfortunately, no longer perfectly matched [16, 1]. More recently, ideas for designing stable PMLs for this problem have emerged from several teams independently. These new approaches, which seem to be very closely related, have been developed for time-dependent applications in [20, 11, 14] and for time-harmonic applications in the present paper. These different works all deal with the case of a parallel flow, which is orthogonal to the layers.

*Received by the editors January 9, 2003; accepted for publication (in revised form) August 15, 2003; published electronically March 3, 2004.
http://www.siam.org/journals/sinum/42-1/42098.html

†Laboratoire POems, UMR 2706 CNRS/ENSTA/INRIA, Institut National de Recherche en Informatique et en Automatique, Domaine de Voluceau, Rocquencourt, BP 105, 78153 Le Chesnay cedex, France (eliane.becache@inria.fr).

‡Laboratoire POems, UMR 2706 CNRS/ENSTA/INRIA, École Nationale Supérieure des Techniques Avancées, 32 boulevard Victor, 75739 Paris cedex 15, France (bonnet@ensta.fr).

§Office National d'Études et de Recherches Aérospatiales, BP 72, 29 avenue de la Division Leclerc, 92322 Châtillon cedex, France. Current address: Laboratoire POems, UMR 2706 CNRS/ENSTA/INRIA, École Nationale Supérieure des Techniques Avancées, 32 boulevard Victor, 75739 Paris cedex 15, France (legendre@ensta.fr).

We are concerned with the propagation of acoustic waves in a duct in the presence of a uniform flow. For such a mean flow, thetime-harmonic linearized Euler equations reduce into a scalar convected Helmholtz equation for the pressure. In this particular case, one could, of course, use a Dirichlet-to-Neumann (DtN) operator to obtain an equivalent problem in a bounded domain. However, the PMLs, being local, are easier to implement, and we intend to extend this method to vectorial cases, involving more general flows in a forthcoming paper.

When applying the *classical* (i.e., Bérenger's) PMLs to the convected Helmholtz equation in a duct, a simple modal analysis shows that the presence of the so-called inverse upstream modes produces an exponential blow-up of the solution in the space variable. This is easy to see, remembering the interpretation of the PMLs as a complex change of variable [8, 24, 10, 9]. This change of variable corresponds to a similarity applied on the axial wave numbers of the modes. For the classical Helmholtz equation, this similarity makes all outgoing modes become evanescent. But in the presence of a flow, the transformation sends the inverse upstream modes into the "bad" part of the complex plane, leading to the instabilities observed in the time domain.

The idea proposed here, which is similar to those developed independently in [20, 14] for time domain applications, consists of applying a translation before the similarity to the axial wave numbers. This removes the unstable modes. We will call the PMLs thus obtained *new* PMLs.

The object of this paper is the analysis of the convergence of both PML models as the thickness of the sponge layer tends to infinity. Similar convergence analyses have already been carried out for the Helmholtz equation, via boundary integral equation techniques in [21] or using the pole condition in [18]. Surprisingly, we prove that, for the convected Helmholtz equation, the two models always converge. In other words, contrary to time domain applications, the presence of unstable modes does not affect the efficiency of the classical PMLs.

Finally, let us emphasize that in most papers concerning PMLs for time-harmonic applications, coefficients are designed in order to satisfy requirements established for time domain applications. We show that this choice is too restrictive: for instance, the particular dependence of these coefficients regarding the frequency has no more justification for the present case.

The outline of this paper is as follows: the equations of the scattering problem are presented in section 2. A formulation in a bounded domain is given, involving DtN conditions on the fictitious boundaries, which are known explicitly through modal expansions. Finally, the well posedness is proven using Fredholm theory.

Classical and new PML techniques, with constant coefficients, are described in section 3. A modal analysis indicates that these layers are "perfectly matched." Besides, they are absorbing, except the classical PMLs in the presence of the so-called inverse upstream modes.

Section 4 is devoted to the analysis of the error due to the truncation of the layers. An equivalent formulation of the problem with PMLs is written in the physical domain, the thickness of the layers appearing in the expression of the DtN maps. In this way, we prove that both PML models converge to the physical solution, as the length of the layers tends to infinity. More precisely, the error in the physical domain does not depend on the PML model under consideration and decreases exponentially fast for both models. Note, however, that classical PMLs lead to an exponentially large solution in the layers, whereas the solution computed with new PMLs is evanescent in the layers.

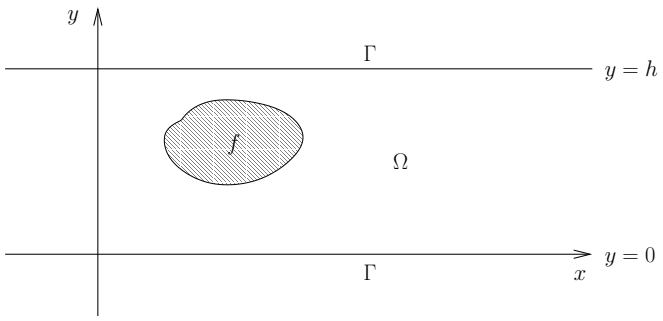


FIG. 1. *The infinite duct.*

Extension to the case of layers with spatially varying coefficients is discussed in section 5, and numerical illustrations are given in the last section.

## 2. The physical and the mathematical models.

**2.1. The problem in the infinite duct.** We consider an infinite rigid duct carrying a mean fluid flow; see Figure 1. The problem is two-dimensional, set in the $xy$-plane, where the $x$- (resp., $y$-) axis is parallel (resp., normal) to the walls of the duct. Mathematically, the duct is defined by the unbounded domain $\Omega = \mathbb{R} \times [0, h]$, where $h$ denotes the distance between the rigid walls.

To describe the propagation of acoustic waves in the duct, we assume the following approximations to be valid:

- The fluid is homogeneous, nonviscous, and nonheat conductive.
- The thermodynamic processes are adiabatic.
- The mean velocity $v_0$ is subsonic and uniform.
- The perturbations are small, and equations are linear in the acoustic quantities.
- A harmonic time dependence $\exp(-i\omega t)$, $\omega > 0$ being the pulsation, is assumed (although this factor is suppressed throughout).

The acoustic pressure field $p(x, y)$ then satisfies the convected Helmholtz equation in the infinite duct:

$$(1 - M^2)\,\frac{\partial^2 p}{\partial x^2} + \frac{\partial^2 p}{\partial y^2} + 2ikM\,\frac{\partial p}{\partial x} + k^2\,p = f \quad \text{in } \Omega, \tag{2.1}$$

where $f \in L^2(\Omega)$ is a compactly supported function and $M = v_0/c_0$ and $k = \omega/c_0$ are, respectively, the Mach number ($-1 < M < 1$) and the wave number, $c_0$ being the sound velocity in the fluid. In addition to (2.1), the pressure satisfies the Neumann homogeneous boundary condition on the two rigid walls of the duct:

$$\frac{\partial p}{\partial y} = 0 \quad \text{on } \Gamma = \partial\Omega. \tag{2.2}$$

To obtain a well-posed problem, a "radiation condition," which selects the "outgoing" waves, needs to be defined at infinity. This condition is nonlocal and is given in terms of the DtN operator. This requires the introduction of the so-called modes of the duct, which are the solutions of (2.1)–(2.2) in the absence of a source ($f = 0$) and with separated variables. These are given by

$$p_n^{\pm}(x, y) = e^{i\beta_n^{\pm} x}\,\varphi_n(y),$$

where

$$\varphi_0(y) = \sqrt{\frac{1}{h}}, \quad \varphi_n(y) = \sqrt{\frac{2}{h}}\,\cos\Big(\frac{n\pi y}{h}\Big), \quad n \in \mathbb{N}^*, \tag{2.3}$$

and where the axial wave numbers $\beta_n^{\pm}$ are the solutions of

$$-(1-M^2)\,\beta^2 - 2kM\,\beta + k^2 = \frac{n^2\pi^2}{h^2}, \quad n \in \mathbb{N}.$$

Let us introduce

$$K_0 = \frac{kh}{\pi\sqrt{1-M^2}}, \tag{2.4}$$

and let $N_0 = [K_0]$ denote the integer part of $K_0$. If $n \le N_0$, $\beta_n^{\pm}$ is real and equal to

$$\beta_n^{\pm} = \frac{-kM \pm \sqrt{k^2 - \frac{n^2\pi^2}{h^2}(1-M^2)}}{1-M^2}. \tag{2.5}$$

In this case, $p_n^{\pm}$ is called a propagative mode. The number of propagative modes is an increasing function of the Mach number $M$, which is assumed to be positive. Simple calculations show that the group velocity $\frac{\partial\omega}{\partial\beta}$ is positive for the $p_n^+$ modes and negative for the $p_n^-$ modes. A well-known effect of the presence of flow is the existence, when

$$\sqrt{1-M^2}\,\frac{n\pi}{h} < k < \frac{n\pi}{h},$$

of modes $p_n^+$ which have a negative phase velocity $\frac{\omega}{\beta}$ and a positive group velocity. These are called inverse upstream modes.

The axial wave number $\beta_n^{\pm}$ is complex if $n > N_0$:

$$\beta_n^{\pm} = \frac{-kM \pm i\sqrt{\frac{n^2\pi^2}{h^2}(1-M^2) - k^2}}{1-M^2}. \tag{2.6}$$

In this case, $p_n^{\pm}$ is exponentially decreasing when $x \to \pm\infty$ and is called an evanescent mode.

**2.2. Reduction to a bounded domain.** We now want to select the outgoing solution (2.1)–(2.2), which corresponds to a superposition of $p_n^+$ (resp., $p_n^-$) modes when $x \to +\infty$ (resp., $x \to -\infty$), i.e., either to the propagative modes with a positive (resp., negative) group velocity or to the evanescent modes.

To derive the appropriate DtN boundary condition, we introduce the bounded domain $\Omega_b$, located in between two boundaries $\Sigma_{\pm}$, respectively, located at $x = x_-$ and $x = x_+$ (see Figure 2), such that the support of the source $f$ is included in $\Omega_b$:

$$\Omega_b = \{(x,y) \in \Omega,\ x_- \le x \le x_+\}.$$

We set $\Omega_{\pm}$ the complementary domains

$$\Omega_- = \{(x,y) \in \Omega,\ x < x_-\} \quad \text{and} \quad \Omega_+ = \{(x,y) \in \Omega,\ x > x_+\}.$$

The solution $p$ of (2.1) then satisfies the homogeneous equation

$$(1-M^2)\,\frac{\partial^2 p}{\partial x^2} + 2ikM\,\frac{\partial p}{\partial x} + \frac{\partial^2 p}{\partial y^2} + k^2\,p = 0 \quad \text{in } \Omega_{\pm} \tag{2.7}$$

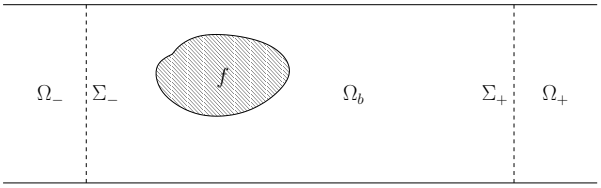


FIG. 2. *The bounded domain.*

and therefore can be decomposed on the modes. Consequently, in $\Omega_-$, i.e., for $x < x_-$, we have

$$p(x,y) = \sum_{n=0}^{+\infty} \left(p(x_-,.),\varphi_n\right)_{L^2(\Sigma_-)}\ \varphi_n e^{i\beta_n^-(x-x_-)},$$

and in $\Omega_+$, i.e., for $x > x_+$,

$$p(x,y) = \sum_{n=0}^{+\infty} \left(p(x_+,.),\varphi_n\right)_{L^2(\Sigma_+)}\ \varphi_n e^{i\beta_n^+(x-x_+)},$$

where $(\cdot,\cdot)_{L^2(\Sigma_+)}$ (resp., $(\cdot,\cdot)_{L^2(\Sigma_-)}$) denotes the $L^2(\Sigma_+)$ (resp., $L^2(\Sigma_-)$) inner product for scalar functions:

$$(u,v)_{L^2(\Sigma_\pm)} \equiv \int_{\Sigma_\pm} u(y)\overline{v}(y)\,\mathrm{d}y.$$

The DtN operators $T_\pm$ can then be defined as

$$\begin{aligned} T_\pm :\ H^{1/2}(\Sigma_\pm) &\to H^{-1/2}(\Sigma_\pm), \\ \phi &\mapsto \mp \sum_{n=0}^{+\infty} i\beta_n^\pm\ (\phi,\varphi_n)_{L^2(\Sigma_\pm)}\ \varphi_n(y), \end{aligned} \tag{2.8}$$

and we have the following boundary conditions on $\Sigma_\pm$ for the solution of (2.1):

$$\frac{\partial p}{\partial \boldsymbol{n}} = -T_\pm p \quad \text{on } \Sigma_\pm, \tag{2.9}$$

where the vector $\boldsymbol{n}$ denotes the unit outward normal to $\Sigma_\pm$.

Having established exact boundary conditions satisfied by $p$, we can now define a problem in the bounded domain $\Omega_b$: find $p \in H^1(\Omega_b)$ such that

$$\begin{cases} (1-M^2)\,\dfrac{\partial^2 p}{\partial x^2} + 2ikM\,\dfrac{\partial p}{\partial x} + \dfrac{\partial^2 p}{\partial y^2} + k^2\,p = f & \text{in } \Omega_b, \\ \dfrac{\partial p}{\partial y} = 0 & \text{on } \Gamma \cap \partial\Omega_b, \\ \dfrac{\partial p}{\partial \boldsymbol{n}} = -T_\pm p & \text{on } \Sigma_\pm. \end{cases} \tag{2.10}$$

The fact that $f$ is compactly supported in $\Omega_b$ shows clearly that problems (2.10) and (2.1)–(2.2) are equivalent in the sense of the following proposition.

PROPOSITION 2.1. *If $p$ is a solution of system* (2.1)–(2.2)*, then $p_{|\Omega_b}$ is a solution of* (2.10)*. Conversely, if $\widetilde{p}$ is a solution of* (2.10)*, then $\widetilde{p}$ can be extended in a unique way to a solution of* (2.1)–(2.2)*.*

**2.3. Well posedness.** Formulation (2.10) has two main advantages. First, from a theoretical point of view, it provides a result of existence and uniqueness of the solution. Second, it can be used to obtain numerical solutions, since it is posed in a bounded domain.

An equivalent weak form of system (2.10) can then be written as follows: find $p \in H^1(\Omega_b)$ such that

$$a_{\Omega_b}(p,q) = -\int_{\Omega_b} f\overline{q}\,\mathrm{d}x\,\mathrm{d}y \quad \forall q \in H^1(\Omega_b), \tag{2.11}$$

where the sesquilinear form $a_{\Omega_b}(\cdot\,,\cdot)$ is defined by

$$a_{\Omega_b}(p,q) = b(p,q) + c(p,q), \tag{2.12}$$

with

$$b(p,q) = \int_{\Omega_b} \left( (1-M^2)\,\frac{\partial p}{\partial x}\frac{\partial \overline{q}}{\partial x} + \frac{\partial p}{\partial y}\frac{\partial \overline{q}}{\partial y} + p\overline{q} \right) \mathrm{d}x\,\mathrm{d}y + \langle T_+ p, q\rangle_{\Sigma_+} + \langle T_- p, q\rangle_{\Sigma_-}\,, \tag{2.13}$$

where the brackets $\langle\cdot,\cdot\rangle_{\Sigma_+}$ (resp., $\langle\cdot,\cdot\rangle_{\Sigma_-}$) denote the natural duality pairing between $H^{-1/2}(\Sigma_+)$ and $H^{1/2}(\Sigma_+)$ (resp., $H^{-1/2}(\Sigma_-)$ and $H^{1/2}(\Sigma_-)$), and

$$c(p,q) = \int_{\Omega_b} \left( -2ikM\,\frac{\partial p}{\partial x}\overline{q} - (1+k^2)\,p\overline{q} \right) \mathrm{d}x\,\mathrm{d}y. \tag{2.14}$$

It was shown in [6] that this problem is of Fredholm type. By the Fredholm alternative, problem (2.11) is well posed if and only if the homogeneous problem has no solution except the trivial one, $p = 0$.

THEOREM 2.2. *The problem is well posed if and only if*

$$k \neq \sqrt{1-M^2}\,\frac{n\pi}{h} \quad \forall n \in \mathbb{N}. \tag{2.15}$$

*Proof.* Suppose that $p$ is a solution of (2.1)–(2.2) with $f = 0$. Then there are complex constants $A_n^+$ and $A_n^-$ such that

$$p(x,y) = \sum_{n=0}^{+\infty} \left( A_n^+\, e^{i\beta_n^+ x} + A_n^-\, e^{i\beta_n^- x} \right) \varphi_n(y),$$

with definitions (2.3) through (2.6). Boundary condition (2.9) then gives

$$A_n^-(\beta_n^- - \beta_n^+) = A_n^+(\beta_n^- - \beta_n^+) = 0$$

so that $p$ vanishes identically if $\beta_n^+ \neq \beta_n^-$ or, likewise, if $k^2 \neq (1-M^2)\,\frac{n^2\pi^2}{h^2}$.

Suppose conversely that $k = \sqrt{1-M^2}\,\frac{n\pi}{h}$; then

$$\beta_n^+ = \beta_n^- = -\frac{kM}{1-M^2},$$

and $\varphi_n(y)\,e^{i\beta_n^+ x}$ is a nontrivial solution of the homogeneous problem. ∎

In what follows, we assume the problem is well posed, which means that (2.15) is satisfied.

**3. The PML model.** The PML model introduced by Bérenger for the time-dependent Maxwell equations can be constructed using a complex change of variable in the frequency domain, as shown in [8, 10, 9]. We use this same approach in the present paper. This is closely related to the technique known as dilation analyticity for the study of resonances [17].

In this section, we briefly recall some properties of the classical PML formulation for the Helmholtz equation. Note that in the context of propagation in a waveguide the interpretation of the method relies on the modal approach instead of the usual plane wave approach. This modal analysis allows us to point out the origin of the instabilities in the presence of flow and leads naturally to the introduction of a new model of PMLs as a remedy.

**3.1. Modal analysis of Bérenger's model in a waveguide.** The purpose of the method is to provide a fictitious, absorbing medium such that its interface with the "physical" bounded domain does not reflect any outgoing mode. Transposing Bérenger's formulation in the frequency domain from its original setting in the time domain consists of making the following substitution:

$$\frac{\partial}{\partial x} \longrightarrow \alpha \, \frac{\partial}{\partial x}, \tag{3.1}$$

where $\alpha$ is a complex function taken to be

$$\alpha(x) = \frac{-i\omega}{-i\omega + \sigma(x)} \tag{3.2}$$

with $\sigma(x)$ a real, positive function such as $\sigma(x) = 0$ (and therefore $\alpha(x) = 1$) in $\Omega_b$, the derivative with respect to $y$ being left unchanged.

In the case of the Helmholtz equation, we obtain

$$\alpha(x) \, \frac{\partial}{\partial x} \left( \alpha(x) \, \frac{\partial p}{\partial x} \right) + \frac{\partial^2 p}{\partial y^2} + k^2 \, p = f \quad \text{in } \Omega. \tag{3.3}$$

Note that the writing of this equation in the weak sense implies the following jump conditions at the interfaces between $\Omega_b$ and the PMLs:

$$[p(x,y)] = 0 \quad \text{and} \quad \left[ \alpha(x) \, \frac{\partial p}{\partial x}(x,y) \right] = 0. \tag{3.4}$$

For the modal analysis in the waveguide, we now assume that $\alpha(x)$ is a constant in $\Omega \setminus \Omega_b$, which we still denote by $\alpha$ for the sake of simplicity. In other words,

$$\alpha(x) = \begin{cases} 1 & \text{if } x_- \leq x \leq x_+, \\ \alpha & \text{otherwise.} \end{cases} \tag{3.5}$$

For any $\alpha$, the interface between the PML and the physical domain is perfectly transparent, and we will see that if $\alpha$ is well chosen, the transmitted waves decrease exponentially in the layer.

Classically, the modes in a waveguide are given by

$$p_n^{\pm}(x,y) = e^{\pm i \beta_n x} \varphi_n(y), \quad n \in \mathbb{N}, \tag{3.6}$$

where functions $\varphi_n$, for all $n \in \mathbb{N}$, are defined by (2.3) and axial wave numbers $\beta_n$ are solutions of the dispersion equation

$$\beta_n{}^2 = k^2 - \frac{n^2 \pi^2}{h^2}, \quad n \in \mathbb{N},$$

such that $\beta_n > 0$ for the propagative modes and $\mathrm{Im}(\beta_n) > 0$ for the evanescent modes. Referring to subsection 2.1, note that

$$\beta_n = \beta_n^+ = -\beta_n^-,$$

with the Mach number $M$ taken equal to zero in the definitions (2.5) and (2.6) of $\beta_n^\pm$. In the same manner, one can define the modes in the PML as

$$p_{n,\alpha}^\pm(x,y) = e^{\pm i\beta_{n,\alpha}x}\varphi_n(y), \quad n \in \mathbb{N}, \tag{3.7}$$

with

$$\beta_{n,\alpha} = \frac{\beta_n}{\alpha}.$$

If $\alpha$ satisfies the hypotheses

$$\mathrm{Re}(\alpha) > 0, \quad \mathrm{Im}(\alpha) < 0, \tag{3.8}$$

then $p_{n,\alpha}^\pm$ is exponentially decreasing as $x \to \pm\infty$ for any $n$ corresponding either to a propagative or to an evanescent mode. It is now straightforward to show that an incident mode $p_n^+$ generates an evanescent transmitted mode $p_{n,\alpha}^+$ in $\Omega_+$ and no reflection at the interface $\Sigma_+$. Let us stress that assumption (3.8) is the only requirement on $\alpha$ to obtain a PML. Surprisingly, the fairly restrictive choice (3.2) seems to be used in most time-harmonic applications.

**3.2. The new PML formulation for the convected Helmholtz equation.** A natural idea for designing a PML for the convected Helmholtz equation, already used in the literature for applications in the time domain, is to apply the technique described in the previous subsection. It has been observed by several authors that this approach leads to instabilities in the time domain [19, 13, 16, 26]. The presence of instabilities have been explained in [2], thanks to an analysis via group velocities. In the context of a duct, this phenomenon can be easily understood using the modal approach.

As in the no-flow case, the axial wave numbers $\beta_{n,\alpha}^\pm$ of the modes $p_{n,\alpha}^\pm$ in the PML are given by

$$\beta_{n,\alpha}^\pm = \frac{\beta_n^\pm}{\alpha}, \quad n \in \mathbb{N}.$$

This can be illustrated by representing the $\beta_n^\pm$ and $\beta_{n,\alpha}^\pm$ in the complex plane. We clearly notice in Figures 3 and 4 that the transformation

$$\begin{array}{rccc} S_\alpha & : & \mathbb{C} & \to & \mathbb{C}, \\ & & z & \mapsto & \dfrac{z}{\alpha}, \end{array}$$

due to the change of variable used in the PML, is a similarity of ratio $\frac{1}{|\alpha|}$ and angle $\arg\left(\frac{1}{\alpha}\right) = -\arg(\alpha)$ around the origin in the complex plane. The main difference between the equation considered here and the Helmholtz equation is the possible existence of inverse upstream modes. Indeed, if $p_n^+$ is an inverse upstream mode (as defined in subsection 2.1), the corresponding $\beta_n^+$ is negative so that $\mathrm{Im}(\frac{\beta_n^+}{\alpha})$ becomes negative for any $\alpha$ satisfying assumption (3.8). This is illustrated in Figure 5, the third propagative downstream mode of the case presented being an inverse upstream

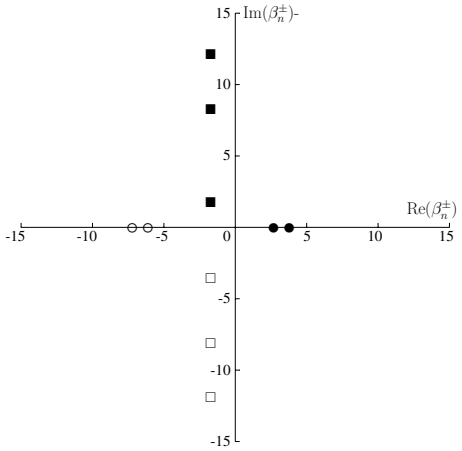


FIG. 3. *First axial wave numbers of the modes for the convected Helmholtz equation ($k = 5$, $M = 0.3$, and $h = 1$). Circles and squares are respectively associated with propagative and evanescent modes, while filled and empty symbols, respectively, refer to downstream and upstream modes.*

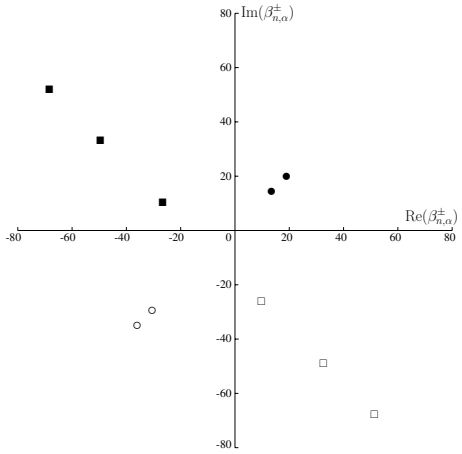


FIG. 4. *Effect of the similarity $S_\alpha$ ($\alpha = 0.1(1-i)$) on the first axial wave numbers of the modes for the convected Helmholtz equation ($k = 5$, $M = 0.3$, and $h = 1$).*

mode. This leads us to the conclusion that the PML model does not produce any unstable (i.e., exponentially growing in the layer) modes if all the axial wave numbers $\beta_{n,\alpha}$ for the propagative downstream (resp., upstream) modes are strictly located in the upper (resp., lower) half of the complex plane.

Guided by the previous geometrical interpretation, we apply a translation in the complex plane prior to the similarity which moves all the $\beta_{n,\alpha}^{+}$'s corresponding to the inverse upstream modes in the right half-plane and keeps the $\beta_{n,\alpha}^{-}$'s associated with propagative modes in the left one. Such a transformation is equivalent to the following substitution in (2.1):

$$\frac{\partial}{\partial x} \longrightarrow \alpha \frac{\partial}{\partial x} + i\lambda$$

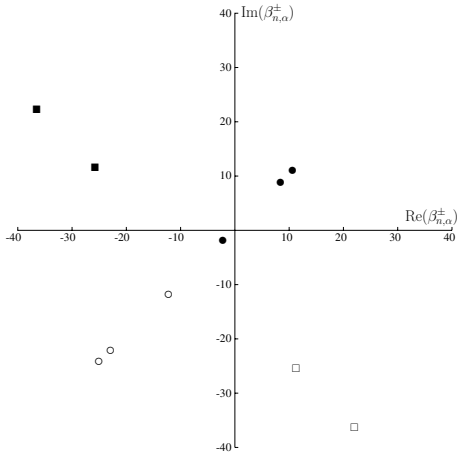


FIG. 5. *Effect of the similarity $S_\alpha$ ($\alpha = 0.2(1-i)$) on the first axial wave numbers of the modes for the convected Helmholtz equation in presence of an inverse upstream mode ($k = 6$, $M = 0.4$, and $h = 1$).*

with $\lambda \in \mathbb{R}$. The resulting axial wave numbers are now given by

$$\beta^{\pm}_{n,\alpha,\lambda} = \frac{\beta^{\pm}_n - \lambda}{\alpha}, \quad n \in \mathbb{N}. \tag{3.9}$$

Although $\lambda$ could be chosen from among several values, the most appropriate choice is the following:

$$\lambda^* = -\frac{kM}{1-M^2}. \tag{3.10}$$

This value corresponds to the real part of the wave number of each evanescent mode, and, for any $\alpha$ satisfying assumption (3.8), the $\beta^{\pm}_{n,\alpha,\lambda^*}$'s are well located. Other choices for $\lambda$ would require further restrictions on $\alpha$ in order to ensure that the $\beta_n$'s associated with evanescent modes also stay in the "good side" of the complex plane (see Figure 6).

We denote in the following by $\lambda(x)$ the function defined by

$$\lambda(x) = \begin{cases} 0 & \text{if } x_- \le x \le x_+, \\ \lambda & \text{otherwise.} \end{cases} \tag{3.11}$$

Finally, the equation in the new PML medium can be written as

$$\left(1-M^2\right)\left(\alpha(x)\,\frac{\partial}{\partial x} + i\lambda(x)\right)^2 p \,+\, \frac{\partial^2 p}{\partial y^2} \,+\, 2ikM\left(\alpha(x)\,\frac{\partial}{\partial x} + i\lambda(x)\right) p \,+\, k^2 p = f \quad \text{in } \Omega, \tag{3.12}$$

where the function $\alpha(x)$ (resp., $\lambda(x)$) is defined in (3.5) (resp., in (3.11)) with $\lambda \in \mathbb{R}$ and $\alpha \in \mathbb{C}$ satisfying assumption (3.8). Writing this equation in a weak sense implies jump conditions at the interfaces between $\Omega_b$ and the layers:

$$[p(x,y)] = 0 \quad \text{and} \quad \left[\alpha(x)\,\frac{\partial p}{\partial x}(x,y) + i\lambda(x)\,p(x,y)\right] = 0. \tag{3.13}$$

*Remark.* This new change of variable can also be used to derive stable PMLs in the time domain, as is done in [20, 14].

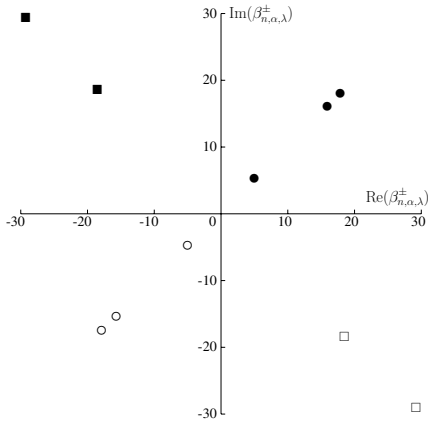


FIG. 6. *Effect of the new transformation (translation prior to similarity $S_\alpha$) on the first axial wave numbers of the modes for the convected Helmholtz equation in the presence of an inverse upstream mode ($k = 6$, $M = 0.4$, and $h = 1$), $\alpha = 0.2(1 - i)$, and $\lambda = -\frac{kM}{1-M^2}$.*

## 4. PML truncation. Error estimates.

**4.1. Truncation of the absorbing layer and well posedness.** Until now, we have considered an absorbing layer of infinite length. In practice, one has to bound the computational domain and layers are of finite length $L$ in this section.

We denote by $\Omega^L$ the truncated domain and by $\Sigma^L_\pm$ the external boundaries, presented in Figure 7. For simplicity, we choose to use homogeneous Dirichlet boundary conditions on these boundaries, but the analysis done in the following would still be valid for the natural boundary conditions $\alpha \frac{\partial p}{\partial x} + i\lambda\, p = 0$. Let $p^L$ denote the solution in the truncated domain, satisfying

$$\begin{cases} \left(1 - M^2\right)\left(\alpha(x)\,\dfrac{\partial}{\partial x} + i\lambda(x)\right)^2 p + \dfrac{\partial^2 p}{\partial y^2} \\ \quad + 2ikM\left(\alpha(x)\,\dfrac{\partial}{\partial x} + i\lambda(x)\right) p + k^2\, p = f & \text{in } \Omega^L, \\ \dfrac{\partial p^L}{\partial y} = 0 & \text{on } \Gamma \cap \partial\Omega^L, \\ p^L = 0 & \text{on } \Sigma^L_\pm. \end{cases} \tag{4.1}$$

Denoting $V_L = \left\{q \in H^1(\Omega^L) \mid q = 0 \text{ on } \Sigma^L_\pm\right\}$, a variational formulation of (4.1) can be written as follows: find $p^L \in V_L$ such that

$$a_{\Omega^L}(p^L, q) = -\int_{\Omega^L} \frac{1}{\alpha}\, f\overline{q}\,\mathrm{d}x\,\mathrm{d}y \;\forall q \in V_L, \tag{4.2}$$

where the sesquilinear form $a_{\Omega^L}(\cdot\,,\cdot)$ is defined by

$$a_{\Omega^L}(p, q) = b_L(p, q) + c_L(p, q),$$

with

$$b_L(p, q) = \int_{\Omega^L} \left((1 - M^2)\alpha\,\frac{\partial p}{\partial x}\frac{\partial \overline{q}}{\partial x} + \frac{1}{\alpha}\,\frac{\partial p}{\partial y}\frac{\partial \overline{q}}{\partial y} + p\overline{q}\right) \mathrm{d}x\,\mathrm{d}y$$

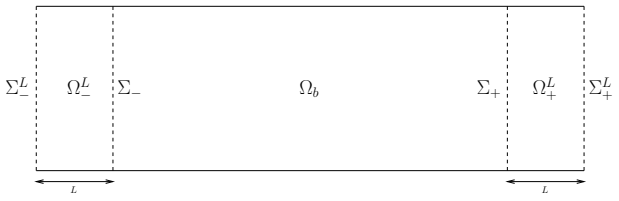


FIG. 7. *The truncated domain* $\Omega^L$.

and

$$\begin{aligned} c_L(p,q) &= \int_{\Omega^L} i\left(\left((M^2-1)\lambda - 2kM\right)\frac{\partial p}{\partial x}\overline{q} + (1-M^2)\lambda\, p\frac{\partial \overline{q}}{\partial x}\right)\mathrm{d}x\,\mathrm{d}y \\ &\quad + \int_{\Omega^L}\left((1-M^2)\frac{\lambda^2}{\alpha} + 2kM\frac{\lambda}{\alpha} - \frac{k^2}{\alpha} - 1\right)p\overline{q}\,\mathrm{d}x\,\mathrm{d}y. \end{aligned}$$

THEOREM 4.1. *If* $\alpha$ *satisfies* (3.8)*, then problem* (4.2) *is of Fredholm type.*

*Proof.* The bounded operator $C_L$ on $H^1(\Omega^L)$, defined by the Riesz representation theorem as

$$(C_L p, q)_{H^1(\Omega^L)} = c_L(p,q)\ \forall (p,q) \in H^1(\Omega^L)^2,$$

is clearly compact (from the compactness of the embedding of $H^1(\Omega^L)$ into $L^2(\Omega^L)$). On the other hand, the sesquilinear form $b_L(\cdot\,,\cdot)$ is coercive on $V_L$. To check this, it suffices to take the real part of $b_L(q,q)$:

$$\begin{aligned} \mathrm{Re}\,(b_L(q,q)) &= \int_{\Omega^L}\left(\mathrm{Re}(\alpha)(1-M^2)\left|\frac{\partial q}{\partial x}\right|^2 + \mathrm{Re}\left(\frac{1}{\alpha}\right)\left|\frac{\partial q}{\partial y}\right|^2 + |q|^2\right)\mathrm{d}x\,\mathrm{d}y \\ &\geq C\,\|q\|^2_{H^1(\Omega^L)}, \end{aligned}$$

where, because of assumption (3.8), $C$ is a strictly positive constant depending on the complex constant $\alpha$ and the Mach number $M$:

$$C = \inf\left((1-M^2)\mathrm{Re}(\alpha), \mathrm{Re}\left(\frac{1}{\alpha}\right), 1\right). \qquad \square$$

**4.2. Reduction to a problem posed in $\Omega_b$.** Remember that our original problem (2.1)–(2.2) has been proved in section 2.2 to be equivalent to the problem (2.10) posed in $\Omega_b$. Having in mind the comparison between the solution $p^L$ of problem (4.1), posed in the truncated domain, and the solution $p$ of the original problem, we first reformulate (4.1) as a problem posed only in $\Omega_b$. Consider the following problem: find $p_b^L \in H^1(\Omega_b)$ such that

$$\text{(4.3)} \qquad \begin{cases} (1-M^2)\,\dfrac{\partial^2 p_b^L}{\partial x^2} + 2ikM\,\dfrac{\partial p_b^L}{\partial x} + \dfrac{\partial^2 p_b^L}{\partial y^2} + k^2\,p_b^L = f & \text{in } \Omega_b, \\ \dfrac{\partial p_b^L}{\partial y} = 0 & \text{on } \Gamma \cap \partial\Omega_b, \\ \dfrac{\partial p_b^L}{\partial \boldsymbol{n}} = -T_\pm^L p_b^L & \text{on } \Sigma_\pm, \end{cases}$$

where $T_\pm^L$ are operators defined as follows:

$$\begin{aligned} T_\pm^L :\ H^{1/2}(\Sigma_\pm) &\to H^{-1/2}(\Sigma_\pm), \\ \phi &\mapsto \mp \sum_{n=0}^{+\infty} i\nu_n^\pm(L)\ (\phi,\varphi_n)_{L^2(\Sigma_\pm)}\ \varphi_n(y), \end{aligned} \tag{4.4}$$

with

$$\nu_n^\pm(L) = \beta_n^\pm + \frac{\beta_n^\mp - \beta_n^\pm}{1 - e^{i(\beta_n^- - \beta_n^+)L/\alpha}}. \tag{4.5}$$

Note that values $\nu_n^\pm(L)$ are well defined, because of assumption (2.15).

PROPOSITION 4.2. *If $p^L$ is a solution of* (4.1)*, then $p^L{}_{|\Omega_b}$ is a solution of* (4.3)*. Conversely, if $p_b^L$ is a solution of* (4.3)*, then it can be extended in a unique way to a solution of* (4.1)*.*

*Proof.* The key idea for reformulating the problem as a problem posed in $\Omega_b$ is to write an exact boundary condition satisfied by the solution on the boundaries $\Sigma_\pm$. We define the complementary domains $\Omega_\pm^L$ by

$$\Omega_-^L = \left\{(x,y)\in\Omega^L,\ x_- - L < x < x_-\right\} \quad \text{and} \quad \Omega_+^L = \left\{(x,y)\in\Omega^L,\ x_+ < x < x_+ + L\right\}.$$

Since $p_\pm^L = p^L{}_{|\Omega_\pm^L}$ satisfies a homogeneous equation in these domains, it can be given as a modal expansion. Consider, for instance, the solution in the right domain $\Omega_+^L$. Using the Dirichlet boundary condition on the external layer boundary $\Sigma_+^L$, the solution can be written as

$$p_+^L(x,y) = \sum_{n=0}^{+\infty} \left(p_+^L(x_+,.),\varphi_n\right)_{L^2(\Sigma_+)} \left(A_n^+\, e^{i\gamma_n^+(x-x_+)} + A_n^-\, e^{i\gamma_n^-(x-x_+)}\right) \varphi_n(y),$$

where we have denoted $\gamma_n^\pm = \beta_{n,\alpha,\lambda}^\pm$, for the sake of clarity, and

$$A_n^\pm = \mp \frac{e^{i\gamma_n^\mp L}}{e^{i\gamma_n^+ L} - e^{i\gamma_n^- L}}.$$

We check easily that these quantities are always defined. Actually, the denominator would vanish if there existed an integer $n$ for which $(\gamma_n^+ - \gamma_n^-)L \in 2\pi\mathbb{Z}$, which means that $(\beta_n^+ - \beta_n^-)L/\alpha \in 2\pi\mathbb{Z}$. If $k^2 \neq (1-M^2)\,\frac{n^2\pi^2}{h^2}$, the quantity $\beta_n^+ - \beta_n^-$ is never zero. Furthermore, with $\alpha$ satisfying assumption (3.8), $(\beta_n^+ - \beta_n^-)L/\alpha$ always has a nonzero imaginary part and thus cannot belong to $2\pi\mathbb{Z}$. We then write an exact boundary condition satisfied by $p_+^L$ on $\Sigma_+$:

$$\left(\frac{\partial p_+^L}{\partial x}\right)_{|\Sigma_+} = \sum_{n=0}^{+\infty} \left(p_+^L(x_+,.),\varphi_n\right)_{L^2(\Sigma_+)} \left(A_n^+\, i\gamma_n^+ + A_n^-\, i\gamma_n^-\right) \varphi_n(y).$$

Using the jump conditions (3.13) and relation (3.9), this yields an exact boundary condition satisfied in the interior by $p_b^L$:

$$\begin{aligned} \left(\frac{\partial p_b^L}{\partial x}\right)_{|\Sigma_+} &= \alpha \left(\frac{\partial p_+^L}{\partial x}\right)_{|\Sigma_+} + i\lambda\, p_{+|\Sigma_+}^L \\ &= i \sum_{n=0}^{+\infty} \left(p_b^L(x_+,.),\varphi_n\right)_{L^2(\Sigma_+)} \left(A_n^+\beta_n^+ + A_n^-\beta_n^-\right) \varphi_n(y). \end{aligned}$$

Setting $\nu_n^+(L) = A_n^+\beta_n^+ + A_n^-\beta_n^-$, this can also be written as

$$\left(\frac{\partial p_b^L}{\partial x}\right)_{|\Sigma_+} = -T_+^L(p_b^L)_{|\Sigma_+},$$

where $T_+^L$ denotes the operator defined in (4.4). ∎

*Remark.* It clearly appears in the expression (4.5) that operators $T_\pm^L$, and thus problem (4.3), do not depend on $\lambda$. In fact, the computed solution $p^L$ depends on $\lambda$ only in the layers.

**4.3. Convergence and error estimates.** We have shown that the original system (2.1)–(2.2) and system (4.1) with absorbing layers of finite length are both equivalent to problems posed only in $\Omega_b$ (respectively, (2.10) and (4.3)). We are now able to compare the solutions of these two problems, which are solutions of the following variational formulations:

For the original problem (2.10): find $p_b \in H^1(\Omega_b)$ such that

$$a_{\Omega_b}(p_b, q) = -\int_{\Omega_b} f\overline{q}\,\mathrm{d}x\,\mathrm{d}y \;\forall q \in H^1(\Omega_b), \tag{4.6}$$

where the sesquilinear form $a_{\Omega_b}(\cdot\,,\cdot)$ is given by (2.12) and can be written as

$$a_{\Omega_b}(p, q) = (Ap, q)_{H^1(\Omega_b)} + \langle T_+ p, q\rangle_{\Sigma_+} + \langle T_- p, q\rangle_{\Sigma_-}\,, \tag{4.7}$$

with $A$ the bounded linear operator on $H^1(\Omega_b)$ defined by

$$(Ap, q)_{H^1(\Omega_b)} = \int_{\Omega_b}\left(\left(1-M^2\right)\frac{\partial p}{\partial x}\frac{\partial \overline{q}}{\partial x} + \frac{\partial p}{\partial y}\frac{\partial \overline{q}}{\partial y} - 2ikM\,\frac{\partial p}{\partial x}\overline{q} - k^2\,p\overline{q}\right)\mathrm{d}x\,\mathrm{d}y. \tag{4.8}$$

For the problem with absorbing layers of finite length (4.3): find $p_b^L \in H^1(\Omega_b)$ such that

$$a_{\Omega_b}^L(p_b^L, q) = -\int_{\Omega_b} f\overline{q}\,\mathrm{d}x\,\mathrm{d}y \;\forall q \in H^1(\Omega_b), \tag{4.9}$$

where the sesquilinear form $a_{\Omega_b}^L(\cdot\,,\cdot)$ can be written as

$$a_{\Omega_b}^L(p, q) = (Ap, q)_{H^1(\Omega_b)} + \left\langle T_+^L p, q\right\rangle_{\Sigma_+} + \left\langle T_-^L p, q\right\rangle_{\Sigma_-}\,, \tag{4.10}$$

the operator $A$ being defined in (4.8).

To prove convergence and get error estimates, we follow an idea developed in [25], which has also been used in [12].

LEMMA 4.3. *Suppose that assumptions* (2.15) *and* (3.8) *hold. Then there exist strictly positive constants* $\mathcal{C} = \mathcal{C}(k, M)$ *and* $\eta = \eta(\theta, k, h, M)$ *(where* $\theta$ *denotes the argument of* $\alpha$*) such that, for all* $(p, q) \in \left(H^1(\Omega_b)\right)^2$*, we have*

$$\left|a_{\Omega_b}(p, q) - a_{\Omega_b}^L(p, q)\right| \le \mathcal{C}e^{-\eta L/|\alpha|}\,\|p\|_{H^1(\Omega_b)}\,\|q\|_{H^1(\Omega_b)}\,. \tag{4.11}$$

*More precisely, the constant* $\eta$ *is determined by*

$$\eta = \frac{2k}{1-M^2}\,\min\left(-\sin(\theta)\sqrt{1-\frac{{N_0}^2}{{K_0}^2}},\ \cos(\theta)\sqrt{\frac{(N_0+1)^2}{{K_0}^2}-1}\right), \tag{4.12}$$

*where* $K_0$ *is defined in* (2.4).

*Proof.* From expressions (4.7) and (4.10), we have

$$a_{\Omega_b}(p,q) - a^L_{\Omega_b}(p,q) = \left(\langle T_+ p, q\rangle_{\Sigma_+} - \langle T^L_+ p, q\rangle_{\Sigma_+}\right) + \left(\langle T_- p, q\rangle_{\Sigma_-} - \langle T^L_- p, q\rangle_{\Sigma_-}\right).$$

Let us focus on the first term in the right-hand side, the estimation of the second one being analogous. From the definitions (2.8) and (4.4) of operators $T_+$ and $T^L_+$, we have, for any $\phi \in H^{1/2}(\Sigma_+)$,

$$\left(T_+ - T^L_+\right)\phi = -\sum_{n=0}^{+\infty} i\left(\beta^+_n - \nu^+_n(L)\right)\,\phi_n\,\varphi_n(y) \quad \text{with } \phi_n = (\phi,\varphi_n)_{L^2(\Sigma_+)}.$$

Therefore, for any $(\phi,\psi) \in (H^{1/2}(\Sigma_+))^2$,

$$\left\langle (T_+ - T^L_+)\phi, \psi\right\rangle_{\Sigma_+} = -\sum_{n=0}^{+\infty} i(\beta^+_n - \nu^+_n(L))\,\phi_n\,\overline{\psi}_n,$$

with $\phi_n = (\phi,\varphi_n)_{L^2(\Sigma_+)}$ and $\psi_n = (\psi,\varphi_n)_{L^2(\Sigma_+)}$. This implies the following estimate:

$$\left|\left\langle \left(T_+ - T^L_+\right)\phi, \psi\right\rangle_{\Sigma_+}\right| \le \sum_{n=0}^{+\infty} \left|\beta^+_n - \nu^+_n(L)\right|\,\left|\phi_n\overline{\psi}_n\right|. \tag{4.13}$$

From (4.5), we have

$$\left|\beta^+_n - \nu^+_n(L)\right| = \frac{|\beta^+_n - \beta^-_n|}{\left|1 - e^{i(\beta^-_n - \beta^+_n)L/\alpha}\right|}.$$

Noticing that, for any $z \in \mathbb{C}$,

$$\left|1 - e^{iz}\right| \ge \left|e^{-\mathrm{Im}(z)} - 1\right|$$

so that, if $\mathrm{Im}(z) < 0$ and $|\mathrm{Im}(z)|$ is large enough, we conclude that this quantity is larger than

$$\left|1 - e^{iz}\right| \ge \left|e^{-\mathrm{Im}(z)} - 1\right| \ge \frac{1}{2}\,e^{-\mathrm{Im}(z)}.$$

We can easily check, using assumption (3.8), that we have $\mathrm{Im}\left((\beta^-_n - \beta^+_n)\,L/\alpha\right) < 0$ for all $n \in \mathbb{N}$ so that, for $L$ large enough, the previous estimate gives us

$$\left|\beta^+_n - \nu^+_n(L)\right| \le 2\left|\beta^+_n - \beta^-_n\right|\,e^{\mathrm{Im}\left((\beta^-_n - \beta^+_n)L/\alpha\right)}. \tag{4.14}$$

Let us now distinguish the two cases.

*The propagative modes $n \le N_0$.* From (2.5), we have

$$\beta^+_n - \beta^-_n = \frac{2k}{1-M^2}\sqrt{1 - \frac{n^2}{{K_0}^2}} = \delta_n > 0.$$

Noting that

$$\delta_{N_0} \le \delta_n \le \frac{2k}{1-M^2},$$

we derive from estimate (4.14)

$$\left|\beta^+_n - \nu^+_n(L)\right| \le 2\delta_n\,e^{-\delta_{N_0} L\,\mathrm{Im}(1/\alpha)} \le \frac{4k}{1-M^2}\,e^{-\delta_{N_0} L\,\mathrm{Im}(1/\alpha)}. \tag{4.15}$$

*The evanescent modes* $n \geq N_0 + 1$. From (2.6), we have

$$\beta_n^+ - \beta_n^- = \frac{2ik}{1-M^2}\sqrt{\frac{n^2}{{K_0}^2} - 1} = i\delta_n, \quad \delta_n > 0.$$

This time, $\delta_n$ is increasing and $\sqrt{\frac{n^2}{{K_0}^2} - 1} \leq \frac{n}{K_0}$. Estimate (4.14) thus yields

$$\left|\beta_n^+ - \nu_n^+(L)\right| \leq \frac{4k}{1-M^2}\frac{n}{K_0}\, e^{-\delta_{N_0+1} L \,\mathrm{Re}(1/\alpha)}. \tag{4.16}$$

By substituting these estimates into (4.13), we see that

$$\begin{aligned}\left|\left\langle \left(T_+ - T_+^L\right)\phi, \psi\right\rangle_{\Sigma_+}\right| \;\leq\; & \frac{4k}{1-M^2}\left(\sum_{n=0}^{N_0} e^{-\delta_{N_0} L \,\mathrm{Im}(1/\alpha)}\, \left|\phi_n\, \overline{\psi}_n\right| \right. \\ & \left. + \sum_{n=N_0+1}^{+\infty} \frac{n}{K_0}\, e^{-\delta_{N_0+1} L \,\mathrm{Re}(1/\alpha)}\, \left|\phi_n \overline{\psi}_n\right|\right).\end{aligned}$$

Setting $\eta = |\alpha| \min(\delta_{N_0} \,\mathrm{Im}(1/\alpha), \delta_{N_0+1}\,\mathrm{Re}(1/\alpha))$, we then have

$$\begin{aligned}\left|\left\langle \left(T_+ - T_+^L\right)\phi, \psi\right\rangle_{\Sigma_+}\right| \;&\leq\; \frac{4k}{1-M^2}\, e^{-\eta L/|\alpha|} \sum_{n=0}^{+\infty}\left(1 + \frac{n^2}{{K_0}^2}\right)^{1/2} \left|\phi_n\, \overline{\psi}_n\right| \\ &\leq\; \mathcal{C}\, e^{-\eta L/|\alpha|}\, |\phi|_{H^{1/2}(\Sigma_+)}\, |\psi|_{H^{1/2}(\Sigma_+)}.\end{aligned}$$

The trace theorem now yields, for any $(p,q) \in \left(H^1(\Omega_b)\right)^2$,

$$\left|\left\langle (T_+ - T_+^L)p, q\right\rangle_{\Sigma_+}\right| \leq \mathcal{C}\, e^{-\eta L/|\alpha|}\, \|p\|_{H^1(\Omega_b)}\, \|q\|_{H^1(\Omega_b)}.$$

One can obviously obtain the same estimate on $\Sigma_-$ and thus conclude the proof of claim (4.11). ∎

Setting $V = H^1(\Omega_b)$, we introduce linear operators $\mathcal{A}$ and $\mathcal{A}^L$ in $\mathcal{L}(V, V')$, respectively, associated with the sesquilinear forms $a_{\Omega_b}(\cdot\,,\cdot)$ and $a^L_{\Omega_b}(\cdot\,,\cdot)$: for all $(p,q) \in V^2$,

$$\langle \mathcal{A}p, q\rangle_{V',V} = a_{\Omega_b}(p,q) \quad \text{and} \quad \left\langle \mathcal{A}^L p, q\right\rangle_{V',V} = a^L_{\Omega_b}(p,q).$$

Obviously estimate (4.11) implies

$$\left\|\mathcal{A} - \mathcal{A}^L\right\|_{\mathcal{L}(V,V')} \leq \mathcal{C}\, e^{-\eta L/|\alpha|}. \tag{4.17}$$

Problems (4.6) and (4.9) can both be written in terms of these operators:

$$\mathcal{A}p_b = -f, \tag{4.18}$$

$$\mathcal{A}^L p_b^L = -f. \tag{4.19}$$

It follows from taking the difference between (4.18) and (4.19) that the error $p_b - p_b^L$ satisfies the following equation:

$$\mathcal{A}^L\left(p_b - p_b^L\right) = \left(\mathcal{A}^L - \mathcal{A}\right) p_b. \tag{4.20}$$

Using estimate (4.17), we are now able to show the following result.

THEOREM 4.4. *Suppose that assumptions* (3.8) *and* (2.15) *hold. There exists* $L_1 > 0$ *such that for all* $L \geq L_1$, $\mathcal{A}^L$ *is an isomorphism on* $H^1(\Omega_b)$ *and the solution* $p_b^L$ *of problem* (4.3) *converges to the solution* $p_b$ *of problem* (2.10). *Furthermore, there exists a constant* $\mathcal{C}$ *depending on* $M$ *and* $k$ *such that*

$$\left\|p_b - p_b^L\right\|_V \leq \mathcal{C}\, e^{-\eta L/|\alpha|} \left\|p_b\right\|_V , \tag{4.21}$$

*with* $\eta$ *being defined in* (4.12).

*Proof.* For $g \in V'$, we consider the following problem: find $u \in V$ such that

$$\mathcal{A}^L u = g. \tag{4.22}$$

We can rewrite the operator $\mathcal{A}^L$ as $\mathcal{A}^L = \mathcal{A} + \left(\mathcal{A}^L - \mathcal{A}\right)$ and, using that $\mathcal{A}$ is an isomorphism on $V$,

$$\mathcal{A}^L = \mathcal{A}\left(I + \mathcal{A}^{-1}\left(\mathcal{A}^L - \mathcal{A}\right)\right).$$

Problem (4.22) thus becomes

$$\left(I + \mathcal{A}^{-1}\left(\mathcal{A}^L - \mathcal{A}\right)\right) u = \mathcal{A}^{-1} g.$$

Applying the Banach fixed point theorem, this problem admits a unique solution if

$$\left\|\mathcal{A}^{-1}\left(\mathcal{A}^L - \mathcal{A}\right)\right\|_{\mathcal{L}(V,V')} < 1,$$

which is satisfied as soon as

$$\left\|\mathcal{A}^L - \mathcal{A}\right\|_{\mathcal{L}(V,V')} < \left\|\mathcal{A}^{-1}\right\|^{-1}_{\mathcal{L}(V,V')}.$$

This can be achieved for $L$ large enough, that is, $L \geq L_1$, since $\left\|\mathcal{A}^L - \mathcal{A}\right\|_{\mathcal{L}(V,V')}$ tends to zero as $L$ tends to infinity, because of (4.17). Moreover, we have

$$\left\|\left(I + \mathcal{A}^{-1}\left(\mathcal{A}^L - \mathcal{A}\right)\right)^{-1}\right\|_{\mathcal{L}(V,V')} < \frac{1}{1 - \left\|\mathcal{A}^{-1}\left(\mathcal{A}^L - \mathcal{A}\right)\right\|_{\mathcal{L}(V,V')}},$$

which implies the following estimate:

$$\left\|u\right\|_V < \frac{\left\|\mathcal{A}^{-1} g\right\|_V}{1 - \left\|\mathcal{A}^{-1}(\mathcal{A}^L - \mathcal{A})\right\|_{\mathcal{L}(V,V')}}.$$

Applying this result to the error, the solution of problem (4.20) yields

$$\begin{aligned}\left\|p_b - p_b^L\right\|_V &< \frac{\left\|\mathcal{A}^{-1}\left(\mathcal{A}^L - \mathcal{A}\right) p_b\right\|_V}{1 - \left\|\mathcal{A}^{-1}\left(\mathcal{A}^L - \mathcal{A}\right)\right\|_{\mathcal{L}(V,V')}} \\ &\leq \frac{\left\|\mathcal{A}^{-1}\right\|_{\mathcal{L}(V,V')} \left\|\mathcal{A}^L - \mathcal{A}\right\|_{\mathcal{L}(V,V')} \left\|p_b\right\|_V}{1 - \left\|\mathcal{A}^{-1}\right\|_{\mathcal{L}(V,V')} \left\|\mathcal{A}^L - \mathcal{A}\right\|_{\mathcal{L}(V,V')}}.\end{aligned}$$

When $\left\|\mathcal{A}^L - \mathcal{A}\right\|_{\mathcal{L}(V,V')}$ is small enough, the quantity in the right-hand side can be bounded by

$$\left\|p_b - p_b^L\right\|_V \leq 2 \left\|\mathcal{A}^{-1}\right\|_{\mathcal{L}(V,V')} \left\|\mathcal{A}^L - \mathcal{A}\right\|_{\mathcal{L}(V,V')} \left\|p_b\right\|_V \leq 2\mathcal{C}\, e^{-\eta} \left\|p_b\right\|_V ,$$

the last inequality coming from (4.17). ∎

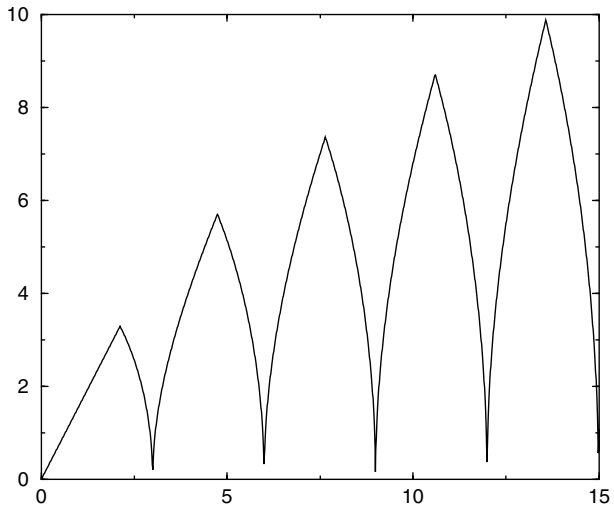


FIG. 8. *Coefficient $\eta$ plotted as a function of wave number $k$ for $M = 0.3$, $h = 1$, and $\theta = -\frac{\pi}{4}$.*

*Remarks.* 1. We emphasize that error estimate (4.21) of Theorem 4.4 does not depend on the parameter $\lambda$. As a consequence, exponential convergence is obtained for both the classical and the new PML models. This is the main difference between the behavior of the new PMLs and that of the classical PMLs in the time domain, as in that case the layers lead to instabilities in the presence of inverse upstream modes [19, 26, 1, 2].

2. Note that estimate (4.21) also proves that convergence holds when the length of the layers $L$ is fixed and $|\alpha|$ tends to 0. This is useful in practice for numerical computations. Indeed, $L$ has to be small in order to reduce the number of degrees of freedom. Moreover, it is more convenient to change the value of parameter $\alpha$ than the length of the layers, which requires a new mesh of the computational domain.

3. The value of $\eta$ is strongly related to the position of wave number $k$ with respect to the cut-off frequencies. More precisely, for a given value of the argument $\theta$ of coefficient $\alpha$, the accuracy deteriorates when $k$ is close to a cut-off wave number (see Figure 8).

**5. Varying coefficients.** In practical computations, it is very common to use a spatially varying coefficient $\alpha(x)$ in the layers. Actually, it has been proven for finite difference schemes that discontinuities in $\alpha$ through the boundaries $\Sigma_\pm$ generate spurious reflections after discretization [10]. In this section, we show that the analysis done previously for constant coefficients $\alpha$ and $\lambda$ can be easily extended to varying coefficients. Let us point out, however, that the numerical results presented in the next section are obtained with constant coefficients and that no significant effects due to the discontinuities have been observed.

Let $\alpha$ and $\lambda$ be two functions of the coordinate $x$, defined from $\mathbb{R}$ to $\mathbb{C}$, such that

$$\alpha(x) = 1 \quad \text{and} \quad \lambda(x) = 0 \quad \text{for } x \in [x_-, x_+].$$

We assume, moreover, that $\alpha(x)$ satisfies (3.8) for all $x > x_+$ or $x < x_-$. Let us consider once more problem (4.1). Since the proof of Theorem 4.1 does not use the fact that $\alpha$ and $\lambda$ are constant in the layers, the theorem still holds, and the problem is of Fredholm type.

To establish a convergence result with respect to the size of the layers, we follow the steps of sections 4.2 and 4.3. The main point is that the modal solutions in the right-hand side layer, for instance, are now

$$p_n^{\pm}(x,y) = \psi_n^{\pm}(x)\varphi_n(y), \quad n \in \mathbb{N},$$

where $\varphi_n$ is given by (2.3) and $\psi_n^{\pm}$ is defined by

$$\begin{cases} \left(\alpha(x)\dfrac{d}{dx} + i\lambda(x)\right)\psi_n^{\pm} = i\beta_n^{\pm}\psi_n^{\pm}, \\ \psi_n^{\pm}(x_+) = 1. \end{cases}$$

It then follows from straightforward calculations that problem (4.1) is equivalent to problem (4.3) set in domain $\Omega_b$, with the following new definition for the coefficient $\nu_n^+(L)$:

$$\nu_n^+(L) = \beta_n^+ + \frac{\beta_n^- - \beta_n^+}{1 - \dfrac{\psi_n^-(x_+ + L)}{\psi_n^+(x_+ + L)}}. \tag{5.1}$$

and a similar definition for $\nu_n^-(l)$. Note, moreover, that

$$\frac{\psi_n^-(x_+ + L)}{\psi_n^+(x_+ + L)} = e^{i(\beta_n^- - \beta_n^+)} \int_{x_+}^{x_+ + L} \frac{1}{\alpha(x)}\,\mathrm{d}x$$

so that again the coefficients $\nu_n^{\pm}(L)$ do not depend on $\lambda$.

The final result then reads as follows.

THEOREM 5.1. *Problem* (4.1) *is well posed, and the solution* $p_b^L$ *of problem* (4.3)*, with* $\nu_n^{\pm}(L)$ *defined above, exists and converges to the solution* $p_b$ *of problem* (2.10) *as* $L \to +\infty$*. Furthermore, there exist three constants* $\mathcal{C} = \mathcal{C}(k, M)$ *and* $\tau_{\pm} = \tau_{\pm}(k, M, \alpha, L)$ *such that*

$$\left\|p_b - p_b^L\right\|_V \leq \mathcal{C}\,\left(e^{-\tau_+} + e^{-\tau_-}\right)\|p_b\|_V\,,$$

*with*

$$\tau_{\pm} = \frac{2k}{1 - M^2}\,\min\left(\mathrm{Im}(I_{\pm})\sqrt{1 - \frac{{N_0}^2}{{K_0}^2}},\ \mathrm{Re}(I_{\pm})\sqrt{\frac{(N_0+1)^2}{{K_0}^2} - 1}\right),$$

*where* $I\pm = \pm\int_{x_\pm}^{x_\pm \pm L} \frac{1}{\alpha(x)}\,\mathrm{d}x$*,* $K_0$ *is defined in* (2.4)*, and* $N_0$ *denotes the integer part of* $K_0$*.*

**6. Numerical results.** In order to illustrate the conclusions previously drawn concerning the PML models, numerical examples are presented. The following configuration is considered: the computational domain is the same as the one presented in Figure 7, extending from $x = -0.2$ to $x = 2.2$ and $y = 0$ to $y = 1$. The layers occupy the region from $x = -0.2$ to $x = 0$ in the downstream direction and from $x = 2$ to $x = 2.2$ in the upstream direction, the thickness $L$ of the layers then being fixed and equal to 10% of the length of domain $\Omega_b$. A compactly supported source $f$ is given by

$$f = \begin{cases} 1 \text{ if } (x-1)^2 + (y-0.7)^2 \leq 0.04, \\ 0 \text{ elsewhere.} \end{cases}$$

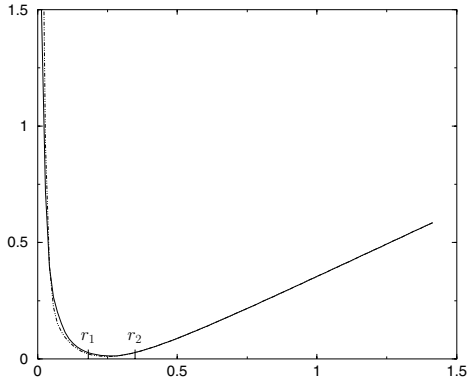


FIG. 9. *Relative error* $\frac{\|p-p_{\rm ref}\|_{H^1(\Omega_b)}}{\|p_{\rm ref}\|_{H^1(\Omega_b)}}$ *as a function of* $|\alpha|$, $k = 10$, *and* $M = 0.3$. *The solid line is the result for the new PML model, while the dotted line refers to the classical PML model.*

The numerical solution of problem (4.2) posed in the domain bounded with PMLs is compared to the computed solution (which is called the *reference solution*) of problem (2.11) posed in the domain bounded with DtN operators. Both approximations are done with a finite element method. The DtN map, usually expressed through an infinite series expansion, is here approximated by truncating the series.

All the simulations have been conducted with the same unstructured mesh, whose mesh size is linked to the problem via a resolution of approximately 20 nodal points per wavelength when using second-order triangular ($P_2$) Lagrange finite elements. For the computation of the reference solution, the number of terms in the truncated DtN map is 8, which is sufficient for accuracy in each of the cases tested. The coefficient $\alpha$ is chosen to be a complex constant in the layers, whose argument is taken to be equal to $-\frac{\pi}{4}$, and coefficient $\lambda$ of the new PML model takes the value $\lambda^*$ defined in (3.10). Homogeneous Dirichlet boundary conditions are imposed on the outer boundaries of the layers. The computations are done with the finite element library MÉLINA [22].

**6.1. The no inverse upstream mode case.** In this first simulation, we choose $k = 10$ and $M = 0.3$. For such values of the wave number and the Mach number, four modes are propagative, and there is no inverse upstream mode. The solution in the layers is then exponentially decaying for both the classical (i.e., $\lambda = 0$) and new PML models.

In Figure 9, the relative error to the reference solution in the $H^1(\Omega_b)$ norm is plotted as a function of the modulus of $\alpha$ for the two models. We observe no noticeable discrepancy between the classical and new PML models, which behave similarly in this case. Both curves present a minimum plateau, and we can roughly distinguish three zones, as indicated in Figure 9:

• $|\alpha| \in [r_1, r_2]$. A very good agreement between the DtN and the PML solutions, for the classical and new PML models, is obtained for a large range of values of $|\alpha|$ corresponding to the plateau seen in Figure 9. The real part of the corresponding solution is shown in Figure 10. We also observe in this figure the effect of the flow on the propagation of sound, as the wavelength of the solution is longer downstream from the source than upstream.

• $|\alpha| > r_2$. For larger values of $|\alpha|$, the layer is insufficiently absorbing, and a reflection occurs at the end of the layers, as shown in Figure 11.

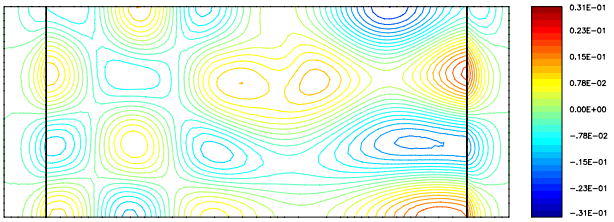


FIG. 10. *Real part of the pressure field;* $k = 10$ *and* $M = 0.3$, $\alpha = .19(1 - i)$, *and* $\lambda = -\frac{kM}{1-M^2}$.

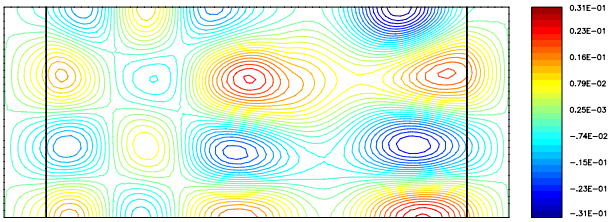


FIG. 11. *Real part of the pressure field;* $k = 10$ *and* $M = 0.3$, $\alpha = 1 - i$, *and* $\lambda = -\frac{kM}{1-M^2}$.

• $|\alpha| < r_1$. For small values of $|\alpha|$, the absorption in the layers is high, but the mesh resolution becomes too coarse to correctly represent modes in the PML medium, thus producing spurious numerical errors, as seen in Figure 12.

We want to confirm the convergence estimate of Theorem 4.4, which implies that

$$-\ln\left(\frac{\left\|p_b - p_b^L\right\|_V}{\|p_b\|_V}\right) \geq \frac{\eta L}{|\alpha|} - \ln(\mathcal{C}).$$

To this end, the opposite of the logarithm of the relative error in $H^1(\Omega_b)$ norm is plotted as a function of the inverse of $|\alpha|$ for both PML models. The exponential convergence of the method, which can be deduced from the slope of curves in Figure 13, agrees satisfactorily with the estimation given by the theory for both PML models, as the two curves coincide for this case.

**6.2. The inverse upstream mode case.** For the choice of $k = 9$ and $M = 0.4$, the last of the four propagative downstream modes (i.e., $n = 3$) has a negative phase velocity and is therefore called an inverse upstream mode. The solution in the downstream layer is then exponentially decreasing or increasing with the distance, depending on the applied PML model. Results for this case are shown in Figures 14 and 15, where the relative error in the $H^1(\Omega_b)$ norm and the opposite of its logarithm, respectively, are shown.

As one can observe in the zoom in Figure 14, the curves of the relative error have again a minimum plateau for both PML models. This time, the size of the plateau is smaller for the classical PML and the error for this model has a rather erratic behavior for small values of $|\alpha|$. The convergence of the method is nonetheless achieved for both models, with the predicted exponential rate (see Figure 15). However, the new PML model seems better suited to practical computations, as one can choose an appropriate and optimal value of $\alpha$ for convergence more conveniently.

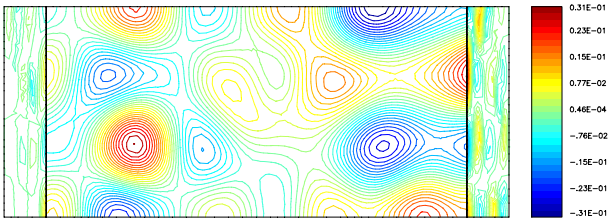


FIG. 12. *Real part of the pressure field;* $k = 10$ *and* $M = 0.3$, $\alpha = .02(1 - i)$, *and* $\lambda = -\frac{kM}{1-M^2}$.

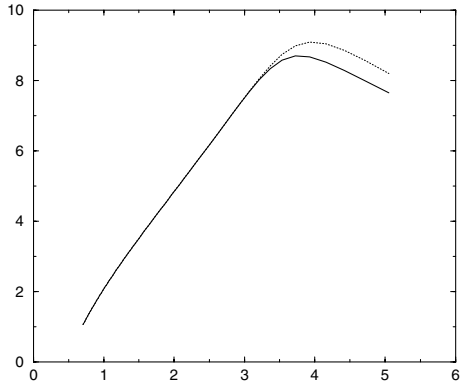


FIG. 13. $-\ln(\frac{\|p-p_{\text{ref}}\|_{H^1(\Omega_b)}}{\|p_{\text{ref}}\|_{H^1(\Omega_b)}})$ *as a function of* $\frac{1}{|\alpha|}$, $k = 10$, *and* $M = 0.3$. *The solid and dotted lines, respectively, refer to results for the new and classical PML models.*

To conclude, Figures 16 and 17, respectively, show the solutions for the new and classical models, the value of $|\alpha|$ for this case corresponding to the minimum of the curves in Figure 14. Note that whatever the behavior of the solution in the layers, the solution in the "physical" domain remains almost the same.

**6.3. Some practical remarks on the use of PMLs for time-harmonic problems.** We would like to point out that the numerical analysis which has been carried out in this section was based on the knowledge of a reference solution. In practice, it would be useful to have a posteriori criteria which indicate whether the numerical solution is satisfactory or not. In transient applications, the quality of the PML model is ensured as soon as the reflections produced at the interface between the physical and the absorbing layer can be neglected. In particular, if the excitation is a pulse localized in time, the exact solution should vanish after a large time, which gives a criterion for evaluating the efficiency of the absorbing layer. The situation is completely different in time-harmonic applications. For instance, we have the following:

- The notion of reflection is more difficult to exploit: as illustrated in the previous numerical results, it is not clear how to distinguish a "reflected" wave from an "incident" wave.
- The experiment of a pulse localized in time has no counterpart in time-harmonic applications.
- A good choice of the absorbing layer parameters allows one to select the outgoing solution of the problem. A bad choice ($\text{Im}(\alpha) > 0$) would select

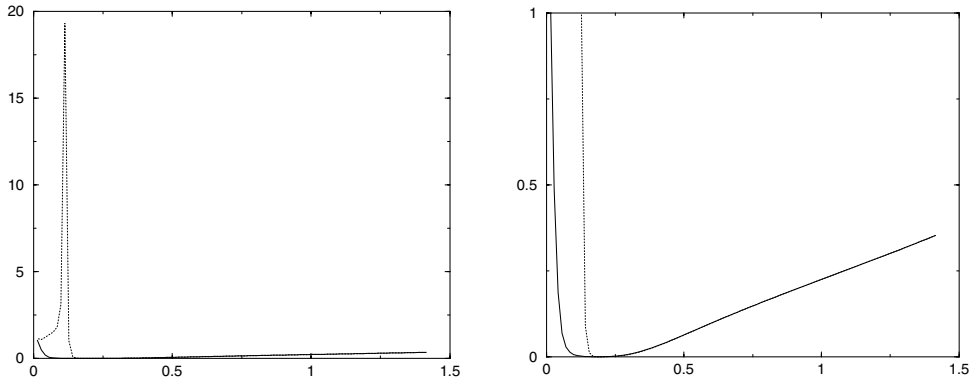


FIG. 14. *Left: relative error* $\frac{\|p-p_{\rm ref}\|_{H^1(\Omega_b)}}{\|p_{\rm ref}\|_{H^1(\Omega_b)}}$ *as a function of* $|\alpha|$, $k = 9$, *and* $M = 0.4$*; right: zoom on the zone of interest. The solid line is the result for the new PML model, while the dotted line refers to the classical PML model.*

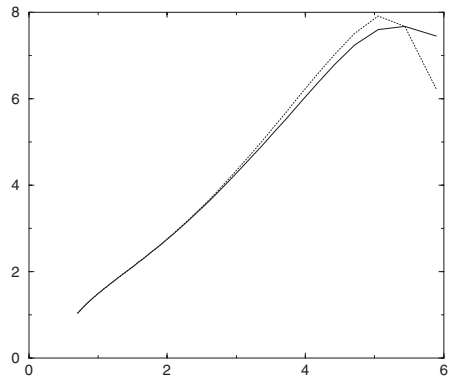


FIG. 15. $-\ln(\frac{\|p-p_{\rm ref}\|_{H^1(\Omega_b)}}{\|p_{\rm ref}\|_{H^1(\Omega_b)}})$ *as a function of* $\frac{1}{|\alpha|}$, $k = 9$, *and* $M = 0.4$. *The solid and dotted lines, respectively, refer to results for the new and classical PML models.*

the ingoing solution, which is difficult to detect when one does not know the exact solution.

- However, one can note that when $|\alpha|$ is too small, spurious numerical errors are observed. They can be removed by refining the mesh in the layer.

**7. Conclusion.** In this paper, we have studied PMLs for the convected Helmholtz equation. In the presence of inverse upstream modes, the solution can have arbitrarily large values in the classical PMLs, thus causing the instabilities observed in time domain applications. We have investigated a new PML model which always leads to an exponentially decreasing solution in the layer, even in the presence of inverse upstream modes. The error analysis surprisingly showed the convergence for both the classical and new models. Nevertheless, numerical results seem to indicate that the error is best controlled with the new model when inverse upstream modes are present. In order to understand the different numerical behaviors of the two models, there remains to analyze the convergence of the solution of the discretized PML models with respect to both the finite element mesh size and the layer parameters $\alpha$ and $L$.

This is a preliminary step in dealing with more complex time-harmonic problems.

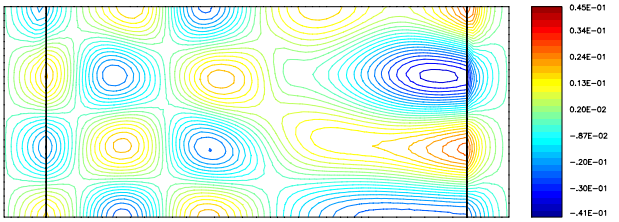


FIG. 16. *Real part of the pressure field;* $k = 9$ *and* $M = 0.4$, $\alpha = .14(1 - i)$, *and* $\lambda = -\frac{kM}{1-M^2}$.

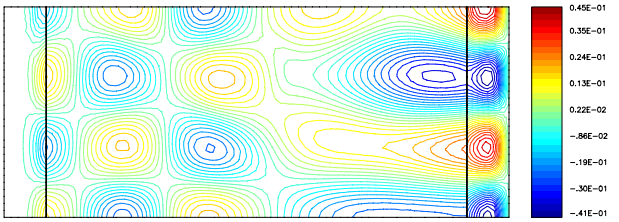


FIG. 17. *Real part of the pressure field;* $k = 9$ *and* $M = 0.4$, $\alpha = .14(1 - i)$, *and* $\lambda = 0$.

In particular, it would be interesting to extend the present method to nonuniform flows. This gives rise to several difficulties. First, even for a parallel flow, the problem can no longer be reduced to a simple scalar equation and has to be modeled with a vectorial model, for instance linearized Euler equations or Galbrun's equation [7]. Furthermore, a modal analysis cannot be done so easily, since the orthogonality of the modes is lost and their completeness is an open question. Finally, for some flows, there exist physical outgoing unstable modes which have to be adequately treated by the absorbing model.

## REFERENCES

[1] S. ABARBANEL, D. GOTTLIEB, AND J. S. HESTHAVEN, *Well-posed perfectly matched layers for advective acoustics*, J. Comput. Phys., 154 (1999), pp. 266–283.
[2] E. BÉCACHE, S. FAUQUEUX, AND P. JOLY, *Stability of perfectly matched layers, group velocities and anisotropic waves*, J. Comput. Phys., 188 (2003), pp. 399–433.
[3] J.-P. BÉRENGER, *A perfectly matched layer for the absorption of electromagnetic waves*, J. Comput. Phys., 114 (1994), pp. 185–200.
[4] J.-P. BÉRENGER, *Three-dimensional perfectly matched layer for the absorption of electromagnetic waves*, J. Comput. Phys., 127 (1996), pp. 363–379.
[5] J.-P. BÉRENGER, *Improved PML for the FDTD solution of wave-structure interaction problems*, IEEE Trans. Antennas and Propagation, 45 (1997), pp. 466–473.
[6] A.-S. BONNET-BEN DHIA, L. DAHI, E. LUNÉVILLE, AND V. PAGNEUX, *Acoustic diffraction by a plate in a uniform flow*, Math. Models Methods Appl. Sci., 12 (2002), pp. 625–647.
[7] A.-S. BONNET-BEN DHIA, G. LEGENDRE, AND E. LUNÉVILLE, *Analyse mathématique de l'équation de Galbrun en écoulement uniforme*, C. R. Acad. Sci. Paris Sér. IIb Méc., 329 (2001), pp. 601–606.
[8] W. C. CHEW AND W. H. WEEDON, *A 3D perfectly matched medium from modified Maxwell's equations with stretched coordinates*, IEEE Microwave Opt. Technol. Lett., 7 (1994), pp. 599–604.
[9] F. COLLINO AND P. MONK, *The perfectly matched layer in curvilinear coordinates*, SIAM J. Sci. Comput., 19 (1998), pp. 2061–2090.
[10] F. COLLINO AND P. B. MONK, *Optimizing the perfectly matched layer*, Comput. Methods Appl. Mech. Engrg., 164 (1998), pp. 157–171.
[11] J. DIAZ AND P. JOLY, *Stabilized Perfectly Matched Layers for Advective Wave Equations*,

manuscript.

[12] D. Gómez Pedreira and P. Joly, *A method for computing guided waves in integrated optics. Part* II: *Numerical approximation and error analysis*, SIAM J. Numer. Anal., 39 (2002), pp. 1684–1711.

[13] J. W. Goodrich and T. Hagstrom, *A Comparison of Two Accurate Boundary Treatments for Computational Aeroacoustics*, AIAA paper 97-1585, 1997.

[14] T. Hagstrom and I. Nazarov, *Absorbing layers and radiation boundary conditions for jet flow simulations*, in Proceedings of the 8th AIAA/CEAS Aeroacoustics Conference, Breckenridge, CO, 2002, AIAA paper 2002-2606.

[15] I. Harari, M. Slavutin, and E. Turkel, *Analytical and numerical studies of a finite element PML for the Helmholtz equation*, J. Comput. Acoust., 8 (2000), pp. 121–137.

[16] J. S. Hesthaven, *On the analysis and construction of perfectly matched layers for the linearized Euler equations*, J. Comput. Phys., 142 (1998), pp. 129–147.

[17] P. D. Hislop and I. M. Sigal, *Introduction to Spectral Theory with Applications to Schrödinger Operators*, Appl. Math. Sci. 113, Springer-Verlag, New York, 1996.

[18] T. Hohage, F. Schmidt, and L. Zschiedrich, *Solving Time-Harmonic Scattering Problems Based on the Pole Condition: Convergence of the PML Method*, Tech. report 01-23, Konrad-Zuse-Zentrum für Informationstechnik Berlin, Berlin, Germany, 2001.

[19] F. Q. Hu, *On absorbing boundary conditions for linearized Euler equations by a perfectly matched layer*, J. Comput. Phys., 129 (1996), pp. 201–219.

[20] F. Q. Hu, *A stable, perfectly matched layer for linearized Euler equations in unsplit physical variables*, J. Comput. Phys., 173 (2001), pp. 455–480.

[21] M. Lassas and E. Somersalo, *On the existence and convergence of the solution of PML equations*, Computing, 60 (1998), pp. 229–241.

[22] D. Martin, *On line documentation of* mélina, http://perso.univ-rennes1.fr/daniel.martin/melina/www/homepage.html.

[23] P. G. Petropoulos, *Reflectionless sponge layers as absorbing boundary conditions for the numerical solution of Maxwell equations in rectangular, cylindrical, and spherical coordinates.*, SIAM J. Appl. Math., 60 (2000), pp. 1037–1058.

[24] C. M. Rappaport, *Perfectly matched absorbing conditions based on anisotropic lossy mapping of space*, IEEE Microwave Guided Wave Lett., 5 (1995), pp. 90–92.

[25] J. Razafiarivelo, *Optimisation de formes en électromagnétisme*, Ph.D. thesis, Université de Paris VI, Paris, France, 1996.

[26] C. K. W. Tam, L. Auriault, and F. Cambuli, *Perfectly matched layer as an absorbing boundary condition for the linearized Euler equations in open and ducted domains*, J. Comput. Phys., 144 (1998), pp. 213–234.

[27] E. Turkel and A. Yefet, *Absorbing PML boundary layers for wave-like equations*, Appl. Numer. Math., 27 (1998), pp. 533–557.

[28] L. Zhao and A. C. Cangellaris, *GT-PML: Generalized theory of perfectly matched layers and its application to the reflectionless truncation of finite-difference time-domain grids*, IEEE Trans. Microwave Theory Tech., 44 (1996), pp. 2555–2563.